JOURNAL OF
Materials
CHEMISTRY

Nickel oxide magnetic nanocomposites in an imine polymer matrix

Cristina Castro, Angel Millan* and Fernando Palacio

Instituto de Ciencia de Materiales de Aragón, Universidad de Zaragoza-C.S.I.C, 50009 Zaragoza, Spain. E-mail: amillan@posta.unizar.es

Received 21st February 2000, Accepted 3rd May 2000

Nanocomposites of nickel(II) oxide in a polyimine matrix have been synthesized by a very simple method. The nickel oxide nanoparticles were precipitated *in situ* within the polymer matrix by drying a polymer–metal complex under mild conditions, without the need for any basic or oxidizing treatment. The polymer–metal complex results from suspending the polymer in a solution of the metal. The size distribution of the nickel oxide nanoparticles contained in the composite shows two different populations with average sizes 12 and 33 nm, respectively. Magnetic susceptibility measurements of the materials reveal the presence of two contributions to the magnetic system. The first has paramagnetic character and arises from the metal-organic matrix. The second consists of frequency-dependent maxima that are typical of superparamagnetic behavior and is related to the presence of nickel oxide nanoparticles.

Introduction

Owing to the unique properties of nanometer-sized particles,[1] there is great interest in the development of suitable methods for their production.[2] For the preparation of nanoparticles, the problem of severely limiting the growth of particles without causing a high size dispersion or particle aggregation must be addressed. A useful technique for achieving this goal is the precipitation of particles inside an organic polymer.[3–9] In addition, the use of organic polymers confers interesting properties on the composite, such as processability, versatility, lightness, optical transparency, resistance to oxidation, *etc.* Of the many applications for nanocomposites, one of the most interesting is in the field of magnetic materials.[10–12] The most common method for the preparation of polymer-based magnetic nanocomposites involves embedding the polymer with a metal salt and then precipitating the metal particles with a reducing agent, or the metal oxide with an oxidizing agent.[3–9] Obviously, to introduce the metal salt precursor inside the polymer matrix, the polymer chain has to contain polar groups, which are normally anionic, such as sulfate,[3] carboxylate,[4] *etc.* Recently, we have presented a method for the preparation of iron oxide and cobalt oxide nanoparticles in nitrogen-based polymers.[13,14] This method has the advantage of using a neutral polymer, furthermore, the metal oxide particles precipitate inside the matrix due to the effect of the imine basicity without the need for any basic or oxidizing agent. It was observed in these experiments that the best results were obtained using the polymer with the highest basicity, highest flexibility and no apolar branches.[13,14] In this work, the same polymer has been successfully used for the production of superparamagnetic nickel oxide nanocomposites. The obtained materials have been characterized by Fourier transform IR spectroscopy, elemental analysis, X-ray powder diffraction and electron microscopy, and their magnetic properties have been characterized.

Experimental and methods

The poly(azomethine) $(C_{13}H_{17}N_3)_n$ was prepared according to previously described methods.[15,16] A typical procedure for the preparation of the polymer–metal complex is as follows: 0.5 g (2.3 mmol of polymer units) of polyimine was suspended in 20 mL of a hot aqueous solution containing 1.15 g (4.5 mmol) of $NiCl_2 \cdot 6H_2O$. The suspension was stirred under reflux for 5 h, filtered and washed with water. An inert atmosphere was maintained throughout the procedure. The resulting polymer complex solid was dried under vacuum at 50 °C for 24 h.

Infrared spectra of samples in KBr pellets were recorded on a Perkin-Elmer 1600 spectrometer. Elemental analysis of C, H and N was carried out on a Perkin-Elmer 248 B microanalyser. The metal content was measured by a plasma 40 ICP Perkin-Elmer spectrometer. The composite material contains 49.6% C, 13.31% N, 6.7% H, and 9.55% Ni.

Susceptibility measurements were performed on a Quantum Design SQUID magnetometer. A JEOL 2000FXIII electron microscope was used for the electron diffraction and TEM observations. Samples were prepared by milling the materials in an agate mortar and placing an acetone suspension of the powders onto a copper grid covered with a Formvar film and coated with carbon. Sample microanalyses were obtained with Link Analytical eXL equipment installed in the electron microscope.

Results and discussion

Materials were prepared according to the method described in the experimental section. The original imine polymer and the polyimine–nickel complex were analyzed by FTIR. The spectrum of the complex shows bands at 3400 and 1626 cm^{-1} that are typical of water of hydration, but does not contain a Cl–Ni band. Thus, it can be inferred that the Cl^- ions do not directly interact with the Ni^{2+} ions and merely compensate for the positive charge of the imine–Ni^{2+} complex. It is observed that the imine stretching band which appears at 1646 cm^{-1} in the original polymer shifts to 1679 cm^{-1} in the spectrum of the polymer complex (Table 1). This can be interpreted in terms of imine–Ni coordination interactions. The formation of polyimine complexes with Fe(II) and Co(II) has been studied before.[17] In that case, the formation of the polyimine–metal complex was also accompanied by a shift of the imine stretching band in the IR spectrum. The structures of both polyimine–metal complexes were examined by EXAFS and found to be nearly octahedral with two tridentate monomeric ligands in perpendicular planes.[17] The structure of the material was described as consisting of polymer chains cross-linked by metal ions. A similar structure can be expected in the present polyimine–Ni(II) complex compound (Fig. 1). The results of the chemical analysis of the samples are shown in

DOI: 10.1039/b001374i

Table 1 Composition and IR data of polyimine (PMH) and polyimine–Ni(II) complex [PMH–Ni(II)] samples

	Elemental analysis		IR bands (cm^{-1})		
Sample	Ni (wt%)	PMH-unit/Ni ratio	$\nu(H_2O)$	ν(C=N)	ν(pyridine)
PMH	—	—	—	1646	1585, 1547
PMH–Ni(II)	9.55	1.95	3422, 1626	1679	1586, 1466

Table 1. The ratio of polymer units per nickel ion is close to 2, in accordance with the coordination number expected for the complex. The pH of the polymer suspension is initially 10 and falls to 6 upon completion of the reaction. This decrease in pH must result from the hydrolysis of Ni solvates when forming the NiO particles. The following equation can be proposed for the formation reaction of the polymer–NiO composite:

$$(1+m)NiCl_2{\cdot}6H_2O+2(C_{13}H_{17}N_3)_n \rightarrow \{[Ni(C_{13}H_{17}N_3)_2]Cl_2{\cdot}4H_2O\}_n+mNiO+(2m)HCl \qquad (1)$$

Fig. 2 shows a TEM micrograph of a polyimine–Ni(II) thin sample. Electrodense regions are observed in the picture which may correspond to inorganic crystalline material. A qualitative EDAX analysis of the particles confirms that they contain a high ratio of Ni atoms (see Fig. 3), in contrast with the light part of the sample. An electron diffraction inspection of light parts in the sample showed an amorphous structure, whereas the dark regions yield patterns that can be indexed on the basis of the pseudocubic unit cell ($a=4.168$ Å) of NiO crystal structure. An example of this pattern is shown in the inset of Fig. 2. Two populations of NiO particles can be distinguished in the image. We have determined the particle size distribution in a sample from more than 500 particles in five different TEM images. This is presented in Fig. 4. Two different particle populations are apparent from the plot: the first shows a maximum at 12 nm, and the second at about 33 nm.

Measurements of the ac magnetic susceptibility at zero external field were carried out over the temperature range 4.2–300 K. The amplitude of the exciting field was 1 Oe and the frequency 100 Hz. A typical plot is represented in Fig. 5. The solid line in the plot results from the fitting of the data to a Curie–Weiss relation[18]

$$\chi=C/(T-\theta) \qquad (2)$$

with parameter values, $C=1.394$ emu K mol^{-1}, $\theta=2$ K. The effective magnetic moment, $\mu_B=3.33$, deduced from the fitted value of the Curie constant, is about the moment expected for a Ni^{2+} ion ($S=1$) in an octahedral crystal field.[19] Thus, the paramagnetic properties of the material can be fully assigned to the polymer–metal complex. On the other hand, in the temperature region between 20 and 40 K, the experimental $\chi'(T)$ curve deviates from a Curie–Weiss relation (eqn. 2). Two peaks around 24 and 33 K appear in this region. It can also be observed from the inset in Fig. 5 that the intensity and the position of the peaks varies with the frequency of the alternating field. This indicates the existence of relaxation phenomena that are usually associated with superparamagnetic

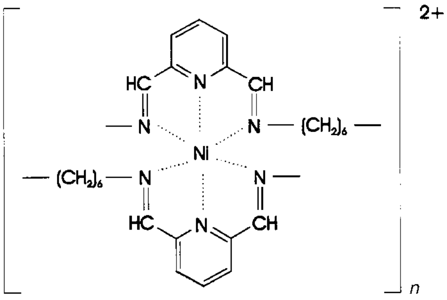

Fig. 1 Expected structure of the polyimine–Ni(II) complex.

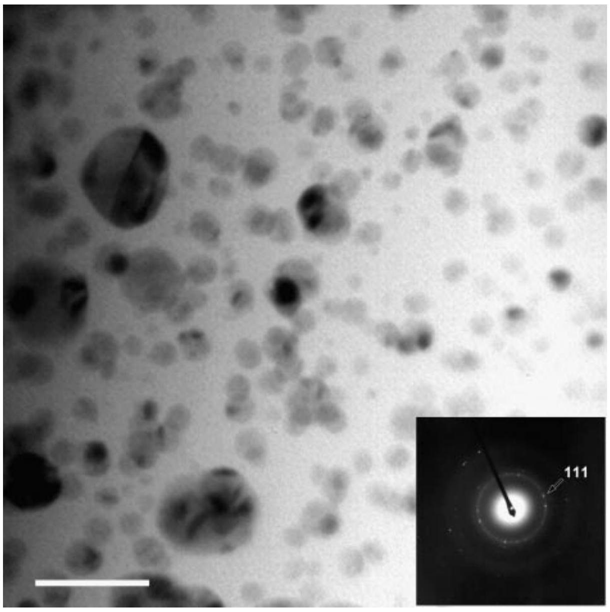

Fig. 2 Texture of the polyimine–Ni(II) composite as observed by TEM; the scale bar at the bottom measures 20 nm. The electron diffraction pattern of a polycrystalline area of the sample that can be indexed on the basis of the NiO unit cell is shown in the inset.

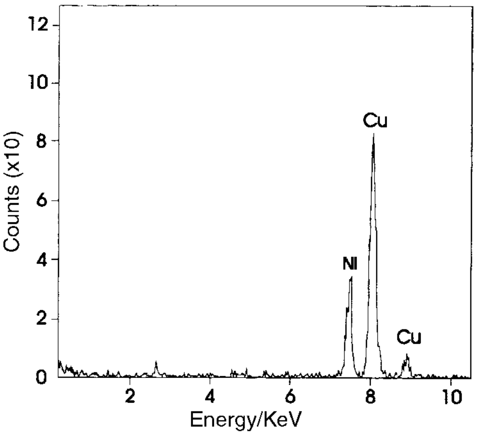

Fig. 3 Microanalysis of selected particles from Fig. 2 (copper peaks are from the sample holder).

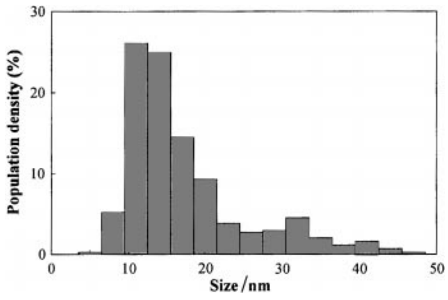

Fig. 4 A histogram plot of the NiO particle size distribution from several TEM images.

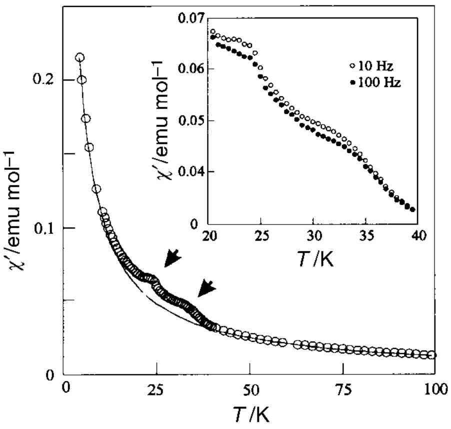

Fig. 5 Temperature dependence of the in-phase component, χ', of the ac susceptibility for a polyimine–NiO composite sample. Inset: variation of $\chi'(T)$ with the exciting frequency.

behavior.[20] A plot of the out-of-phase susceptibility, χ'', *versus* temperature is represented in Fig. 6. The existence of non-zero values of χ'' in the temperature range of the deviation from the Curie–Weiss relation (eqn. 2) confirms the superparamagnetism of the sample.[21] The $\chi''(T)$ curve also shows two maxima at temperatures close to those found in the $\chi'(T)$ plot. The superparamagnetic contribution to the magnetic properties of the composite can be attributed to the nanometric nickel oxide particles contained in the material. The appearance of two peaks in the $\chi'(T)$ and $\chi''(T)$ curves can be related to the presence of two particle populations with a different average size, as observed by TEM. Nickel oxide is an antiferromagnetic compound with a Neel temperature of 523 K. However, it has been demonstrated that for a size below 100 nm, NiO particles exhibit superparamagnetic relaxation phenomena like many ferromagnetic materials.[22] The origin of this behavior has been attributed to residual magnetic moment due to an incomplete magnetic compensation between the two antiferromagnetic sublattices.[23] Moreover, this weak ferromagnetism is also produced by surface effects that acquire an increasing relevance as the particle size decreases. In this way, the permanent moment shown by the NiO nanoparticles must be inversely proportional to the particle size.[22] On the other hand, the temperature of the magnetic susceptibility maximum, known as the blocking temperature, decreases with the particle volume.[21] Therefore, the lower temperature peak of the magnetic susceptibility curve must correspond to the smaller particle population.

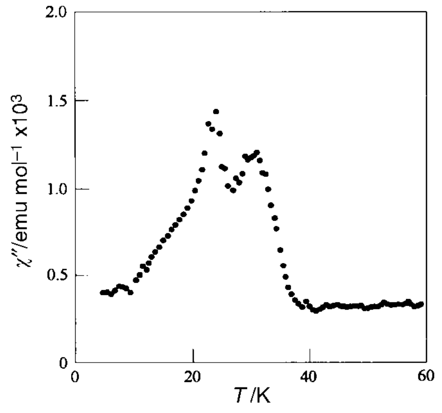

Fig. 6 Temperature dependence of the out-of-phase component, χ'', of the ac susceptibility for a polyimine–NiO composite sample.

Conclusions

Magnetic nickel oxide nanocomposites have been produced from imine polymers by a method that has already been applied with success to the fabrication of iron oxide and cobalt oxide nanocomposites. The procedure for the preparation of the nanocomposite is very simple as compared to the usual methods for the *in situ* production of magnetic nanoparticles in organic polymers, because the imine groups provide the basic medium for the hydrolysis of the metal ions without the need of basic or oxidizing treatments. Two different NiO particle populations are formed in the matrix with average sizes of 12 and 33 nm, respectively. The magnetic properties of the composite are the result of a paramagnetic contribution due to the polymer–metal complex and a superparamagnetic contribution due to NiO nanoparticles contained in the composite.

Acknowledgements

Thanks to Professor A. Larrea and E. Martinez for their assistance with the EM and SQUID magnetometer measurements. Financial support from CICYT (MAT97-0951) is gratefully acknowledged.

References

1 Y. Volokitin, J. Sinzig, L. J. Dejongh, G. Schmid, M. N. Vargaftik and I. I. Moiseev, *Nature*, 1996, **384**, 621; M. L. Bilas, A. Chatelain and W. A. de Heer, *Science*, 1994, **265**, 1682.
2 D. Awschalom and D. DiVicenzo, *Phys. Today*, April 1995 43.
3 R. F. Ziolo, E. P. Giannelis, B. A.; Weinstein, M. P. O'Horo, B. N. Ganguli, V. Mehrotra, M. W. Russell and D. R. Huffman, *Science*, 1992, **257**, 219.
4 Y. Ng. Cheong Chan, G. S. W. Craig, R. R. Schrock and R. E. Cohen, *Chem. Mater.*, 1992, **4**, 885.
5 M. T. Nguyen and A. F. Díaz, *Adv. Mater.*, 1994, **6**, 858.
6 L. Raymond, J.-F. Revol, D. H. Ryan and R. H. Marchessault, *Chem. Mater.*, 1994, **6**, 249.
7 B. H. Sohn and R. E. Cohen, *Chem. Mater.*, 1997, **9**, 264.
8 M. E. Wosniak, A. Sen and A. L. Rheingold, *Chem. Mater.*, 1992, **4**, 753.
9 C. S. Cho, Y. I. Jeong, T. Ishihara, R. Takei, J. U. Park, K. H. Park, A. Maruyama and T. Akaike, *Biomaterials*, 1997, **18**, 323.
10 S. W. Charles and J. Popplewell, in *Ferromagnetic Materials*, ed. E. P. Wohlfarth, North-Holland, Amsterdam, 1980, vol. 2, p. 509.
11 I. Anton, I. De Sabata and L. Vekas, *J. Magn. Magn. Mater.*, 1990, **85**, 219.
12 H. N. Bertran, *Theory of Magnetic Recording*, Cambridge University Press, Cambridge, 1994.
13 F. Palacio, C. Castro, J. Reyes, G. Sturgeon, F. J. Lázaro and J. González-Calbet, *NATO ASI Ser., Ser. C*, 1992, **374**, 793.
14 A. Millan and F. Palacio, *Appl. Organomet. Chem.*, 2000, in press.
15 F. Lions and K. V. Martin, *J. Am. Chem. Soc.*, 1957, **79**, 2733.
16 K. Suetrnatsu, K. Nakarnura and J. Takedi, *Polym. J.*, 1983, **15**, 71.
17 J. García, J. Chaboy, V. Marguin, C. Castro, J. Ramos and F. Palacio, *Jpn. J. Appl. Phys.*, 1993, **32**, 800.
18 A. H. Morrish, *The Physical Properties of Magnetism*, John Wiley & Sons, New York, 1965.
19 R. L. Carlin, *Magnetochemistry*, Springer Verlag, New York, 1986.
20 D. Fiorani, in *The Time Domain in Surface and Structural Dynamics*, ed. G. Long and F. Grandjean, Kluwer Academic Publishers, Dordrecht, 1988, p. 391.
21 F. Palacio, in *Localized and Itinerant Molecular Magnetism. From Molecular Assemblies to the Devices*, ed. E. Coronado, P. Delhaes, D. Gatteschi and J. S. Miller, Kluwer Academic Publishers, Amsterdam, 1996, p. 5.
22 J. T. Richardson, D. I. Yiagas, B. Turk and K. Forster, *J. Appl. Phys.*, 1991, **70**, 6977.
23 L. Neel, *Compt. Rend*, 1961, **252**, 4075.